Transient and late time attractor tachyon dark energy: Can we distinguish it from quintessence?

Amna Ali,* M. Sami,† and A. A. Sen‡

Centre of Theoretical Physics, Jamia Millia Islamia, New Delhi-110025, India

(Received 16 April 2009; published 4 June 2009)

The string inspired tachyon field can serve as a candidate of dark energy. Its equation of state parameter w varies from 0 to -1. In the case of tachyon field potential $V(\phi) \rightarrow 0$ slower (faster) than $1/\phi^2$ at infinity, dark energy (dark matter) is a late time attractor. We investigate the tachyon dark energy models under the assumption that w is close to -1. We find that all the models exhibit unique behavior around the present epoch which is exactly the same as that of the thawing quintessence.

DOI: 10.1103/PhysRevD.79.123501 PACS numbers: 98.80.Cq

I. INTRODUCTION

One of the most challenging problems of modern cosmology is associated with late time acceleration of the Universe which is supported by observations of complementary nature. According to the standard lore, an exotic perfect barotropic fluid with large negative pressure dubbed *dark energy* can account for a repulsive effect causing acceleration [1–3]. The simplest example of dark energy is provided by the cosmological constant Λ. The model is consistent with observation but is plagued with difficult theoretical issues. The field theoretic understanding of Λ is far from being satisfactory and its small numerical values give rise to problems of *fine-tuning* and *coincidence*. A variety of scalar field models including quintessence, tachyons, phantoms, and K-essence has been investigated in recent years to address the problem [2,4,5]. These models have some advantage over the cosmological constant: (i) They can mimic the cosmological constant at the present epoch and can give rise to other observed values of the equation of state parameter w (recent data indicate that w lies in a narrow strip around $w = w_\Lambda = -1$ and is consistent with being below this value). (ii) They can alleviate the fine-tuning and coincidence problems.

The scalar field model, which is the simplest generalization of the cosmological constant, is one with a linear potential [6]. This model starts with a cosmological constant-like behavior where the scalar field is frozen initially due to Hubble damping. Later on, it starts rolling, but because the potential has no minimum, it leads to a collapsing universe in the future. Hence the universe in this model, has a finite history.

The more complicated scalar field models can broadly be classified into two categories. Models in which the scalar field mimics the background (radiation/matter) being subdominant for most of the evolution history. Only at late times it becomes dominant and accounts for the late time acceleration. Such a solution is referred to as *tracker*. In this case $w(\phi) \simeq w_b$ ($w_b = 0, 1/3$) before the transition from a matterlike regime or *scaling regime* to accelerated expansion. Tracker models are independent of initial conditions used for field evolution but do require the tuning of the slope of the scalar field potential. During the scaling regime the field energy density is of the same order of magnitude as the background energy density.

In the second class of models, trackers are absent. Hence at early times, the field gets locked ($w(\phi) = -1$) due to large Hubble damping and waits for the matter energy density to become comparable to field energy density which is made to happen at late times. The field then begins to evolve toward larger values of $w(\phi)$ starting from $w(\phi) = -1$. In this case, for a viable cosmic evolution, one chooses $\rho_\phi \sim \rho_\Lambda$ during the locking regime which requires the tuning of initial conditions of the field. The two classes of scalar fields are called freezing and thawing models.

In the case of a standard scalar field (quintessence), there is a variety of models which possess tracker solutions. In the case of a tachyon field [7,8] (motivated by string theory), there exists no solution which can mimic a scaling matter/radiation regime [9–17]. These models necessarily belong to the class of thawing models. Tachyon models do admit scaling solution in the presence of a hypothetical barotropic fluid with negative equation of state. Tachyon fields can be classified by the asymptotic behavior of their potentials for large values of the field: (i) $V(\phi) \rightarrow 0$ faster than $1/\phi^2$ for $\phi \rightarrow \infty$. In this case dark matterlike solution is a late time attractor. Dark energy may arise in this case as a transient phenomenon. (ii) $V(\phi) \rightarrow 0$ slower than $1/\phi^2$ for $\phi \rightarrow \infty$; these models give rise to dark energy as late time attractor. The two classes are separated by $V(\phi) \sim 1/\phi^2$ which is a scaling potential with $w(\phi) = \text{const}$.

Since observationally, the equation of state parameter of dark energy is very close to 1, we can use this information to simplify the dynamics. In the case of thawing quintessence and phantom field, it allows one to obtain a generic expression for w which represents the entire class of quintessence and phantom models [18,19]. In this paper we apply the same technique to a tachyon field which belongs to the class of thawing models. With the current state of

*amnaalig@gmail.com
†sami.ctp@jmi.ac.in
‡anjan.ctp@jmi.ac.in

observation, we address the issue of distinguishing the tachyon dark energy from the case of quintessence.

II. DYNAMICS OF TACHYON FIELD

In what follows we shall be interested in the cosmological dynamics of the tachyon field which is specified by the Dirac-Born-Infeld (DBI) type of action given by

$$\mathcal{S} = \int -V(\phi)\sqrt{1-\epsilon\partial^{\mu}\phi\partial_{\mu}\phi}\sqrt{-g}d^4x, \quad (1)$$

where on phenomenological grounds, we shall consider a wider class of potentials satisfying the restriction that $V(\phi)\to 0$ as $\phi\to\infty$. The parameter $\epsilon = \pm 1$ where the plus sign corresponds to the normal tachyon field which is nonphantom whereas, with minus sign, one can model phantom type tachyon fields phenomenologically. In Friedman-Robertson-Walker background, the pressure and energy density of ϕ are given by

$$p_\phi = -V(\phi)\sqrt{1-\epsilon\dot{\phi}^2}, \quad (2)$$

$$\rho_\phi = \frac{V(\phi)}{\sqrt{1-\epsilon\dot{\phi}^2}}. \quad (3)$$

The equation of motion which follows from (1) is

$$\ddot{\phi} + 3H\dot{\phi}(1-\epsilon\dot{\phi}^2) + \epsilon\frac{V'}{V}(1-\epsilon\dot{\phi}^2) = 0, \quad (4)$$

where H is the Hubble parameter

$$H^2 = \frac{\rho_\phi + \rho_b}{3}. \quad (5)$$

The evolution equation can be cast in the following autonomous form for convenient use:

$$x' = -(1-\epsilon x^2)(3x - \sqrt{3}\epsilon\lambda y) \quad (6)$$

$$y' = \frac{y}{2}\left[-\sqrt{3}\lambda xy - \frac{3(\gamma_b - \epsilon x^2)y^2}{\sqrt{1-\epsilon x^2}} + 3\gamma_b\right] \quad (7)$$

$$\lambda' = -\sqrt{3}\lambda^2 xy\left(\Gamma - \frac{3}{2}\right) \quad (8)$$

with

$$x = \dot{\phi}, \qquad y = \frac{\sqrt{V(\phi)}}{\sqrt{3}H}, \qquad \lambda = -\frac{V_\phi}{V^{3/2}}, \qquad \Gamma = V\frac{V_{\phi\phi}}{V_\phi^2}, \quad (9)$$

where the prime denotes the derivative with respect to $\ln(a)$. Here γ_b is defined as $p_b = (\gamma_b - 1)\rho_b$ for the background field. In our subsequent calculations, we shall assume a nonrelativistic matter for our background field for which $\gamma_b = 1$.

An important remark on the autonomous system is in order. Let us consider the inverse power law type potential $V(\phi) = V_0\phi^n$ ($n < 0$). Equation (9) tells us that $\Gamma > 3/2$ if $n < -2$ allowing λ to increase monotonously for large values of the field. In this case $\dot{\phi}\to 1$ or $w \to 0$ where as w approaches the de Sitter limit for $n > -2$ ($\Gamma < 3/2$). These two classes of tachyon potentials are separated by the inverse square potential with constant λ ($\Gamma = 3/2$) which provides the analog of scaling potential in the case of a tachyon. However, there is a major difference that in the present case, the field can only mimic a hypothetical fluid with negative equation of state leading to accelerated expansion. Unfortunately, the mass scale in the potential turns out be larger than the Planck mass. The class of potentials designated by $-2 < n < 0$ is free from this problem and gives rise to dark energy as a late time attractor of dynamics. In the analysis to follow, it will be convenient to use the following quantities:

$$\Omega_\phi = \frac{y^2}{\sqrt{1-\epsilon x^2}}, \qquad \gamma_\phi = \epsilon(1+w) = \epsilon^2\dot{\phi}^2, \quad (10)$$

where $w = \frac{p_\phi}{\rho_\phi}$ is the equation of state for the tachyon field. One can now express the autonomous equations through them:

$$\gamma'_\phi = -6\gamma_\phi(1-\epsilon\gamma_\phi) + 2\sqrt{3\gamma_\phi\Omega_\phi}\lambda(1-\epsilon\gamma_\phi)^{5/4} \quad (11)$$

$$\Omega'_\phi = 3\Omega_\phi(1-\epsilon\gamma_\phi)(1-\Omega_\phi) \quad (12)$$

$$\lambda' = -\epsilon\sqrt{3\gamma_\phi\Omega_\phi}\lambda^2(1-\epsilon\gamma_\phi)^{1/4}\left(\Gamma - \frac{3}{2}\right). \quad (13)$$

The first two equations can be combined into one by a change of variable from $a \to \Omega_\phi$

$$\frac{d\gamma_\phi}{d\Omega_\phi} = \frac{\gamma'_\phi}{\Omega'_\phi} = \frac{-2\gamma_\phi(1-\epsilon\gamma_\phi)}{\Omega_\phi(1-\Omega_\phi)(1-\epsilon\gamma_\phi)} + \frac{2\sqrt{3\gamma_\phi\Omega_\phi}\lambda(1-\epsilon\gamma_\phi)^{5/4}}{3\Omega_\phi(1-\Omega_\phi)(1-\epsilon\gamma_\phi)}. \quad (14)$$

A. Late time evolution

From Eq. (14), one can see that for nonphantom and phantom cases, i.e. $\epsilon = \pm 1$, the equation is completely different and hence one expects to have different evolutions for $\gamma_\phi(\Omega_\phi)$ for nonphantom and phantom cases.

But we are interested in the investigations of cosmological dynamics around the present epoch where $\gamma_\phi \ll 1$. Secondly, in our case $w(\phi)$ improves slightly beginning from the locking regime, thereby, telling us that the slope of the potential does not change appreciably. This implies that the potential is very flat around the present epoch such that

$$\frac{1}{V}\left(\frac{V_{,\phi}}{V}\right)^2 \ll 1, \qquad \frac{V_{\phi\phi}}{V^2} \ll 1. \tag{15}$$

In the case of a field domination regime, the two conditions in Eq. (15) define the slow-roll parameters which allows one to neglect the $\ddot{\phi}$ term in the equation of motion for ϕ. In the present context, unlike the case of inflation, the evolution of the field begins in the matter dominated regime and, even today, the contribution of matter is not negligible. The traditional slow-roll parameters cannot be connected to the conditions on the slope and the curvature of the potential which essentially requires that Hubble expansion is determined by the field energy density alone. Thus the slow-roll parameters are not that useful in the case of late time acceleration, though Eq. (15) can still be helpful. In view of the aforesaid, we can drop all the terms of order higher than γ_ϕ in Eq. (14) and assume that the slope of the potential is constant $\lambda = \lambda_0$. These follow from the two slow-roll conditions (15) as we shall show later. The evolution equation then simplifies to

$$\frac{d\gamma_\phi}{d\Omega_\phi} = \frac{-2\gamma_\phi}{\Omega_\phi(1-\Omega_\phi)} + \frac{2\lambda_0}{\sqrt{3}}\frac{\gamma_\phi^{1/2}}{(1-\Omega_\phi)\sqrt{\Omega_\phi}}. \tag{16}$$

Let us note that Eq. (16) is the same as its counterpart in case of quintessence though the full Eq. (14) is different. The difference between tachyon and quintessence dynamics is represented by terms of higher order than γ_ϕ. Thus if we restrict our investigation of dark energy dynamics very close to cosmological constant behavior, we cannot distinguish tachyon dark energy from quintessence. Also Eq. (16) is independent of ϵ. Hence $(1 + w)$ for the nonphantom case and $-(1 + w)$ for the phantom case have identical evolution around the cosmological constant.

Equation (16) can be transformed into a linear differential equation with the change of variable $s^2 = \gamma_\phi$, and we have boundary condition $\gamma_\phi = 0$ at $\Omega_\phi = 0$. The resulting solution expressed in terms of $w(\phi)$

$$\begin{aligned} 1 + w &= \epsilon\frac{\lambda_0^2}{3}\left[\frac{1}{\sqrt{\Omega_\phi}} - \left(\frac{1}{\Omega_\phi} - 1\right)\tanh^{-1}\sqrt{\Omega_\phi}\right]^2 \\ &= \epsilon\frac{\lambda_0^2}{3}\left[\frac{1}{\sqrt{\Omega_\phi}} - \frac{1}{2}\left(\frac{1}{\Omega_\phi} - 1\right)\ln\left(\frac{1+\sqrt{\Omega_\phi}}{1-\sqrt{\Omega_\phi}}\right)\right]^2. \end{aligned} \tag{17}$$

Under the approximation $\gamma_\phi \ll 1$ which is justified about the present epoch, all the tachyon models follow a general track irrespective of the particular field potential. One can see from (17) that $1 + w \sim O(\lambda^2)$. Hence the first slow-roll condition ($\lambda \ll 1$) ensures that $1 + w \ll 1$. We can quantify our second assumption that the slope of the potential does not change appreciably during the evolution as $\lambda'/\lambda \ll 1$. Noting that $\gamma \sim \lambda^2$ and also $\gamma \ll 1$, one can then use Eq. (13) to write

$$\frac{V''}{V^2} - \frac{3}{2}\frac{V'^2}{V^3} \ll 1; \tag{18}$$

together with the first slow-roll condition, this ensures that the second slow-roll condition is satisfied. We also show in Fig. 1 the actual behavior of λ for different potentials for the nonphantom case. This also shows λ is constant during the entire evolution for all practical purposes. One also arrives at the same behavior for the phantom case. In Figs. 2 and 3 we show our analytical approximation for $w(\Omega_\phi)$ in comparison with the numerical solutions of the exact equations for different potentials with different initial values for λ for nonphantom and phantom cases. They show that our approximation works reasonably well as long as λ_0 is small, i.e. as long as the slow-roll conditions are satisfied.

Next, we can use Eq. (12) to solve for $\Omega_\phi(a)$ to determine $w(a)$. Assuming $\gamma_\phi \ll 1$, this gives

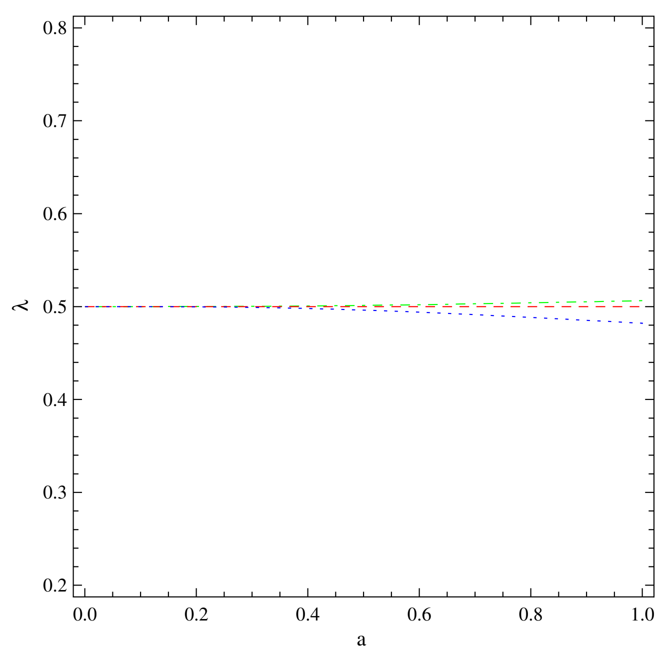

FIG. 1 (color online). Behavior of λ as a function of scale factor for different potentials. We have chosen the initial value of $\lambda_i = 0.5$. The dotted, dashed, and dot-dashed curves correspond to $V(\phi) = \phi^{-1}$, ϕ^{-2}, and ϕ^{-3} respectively.

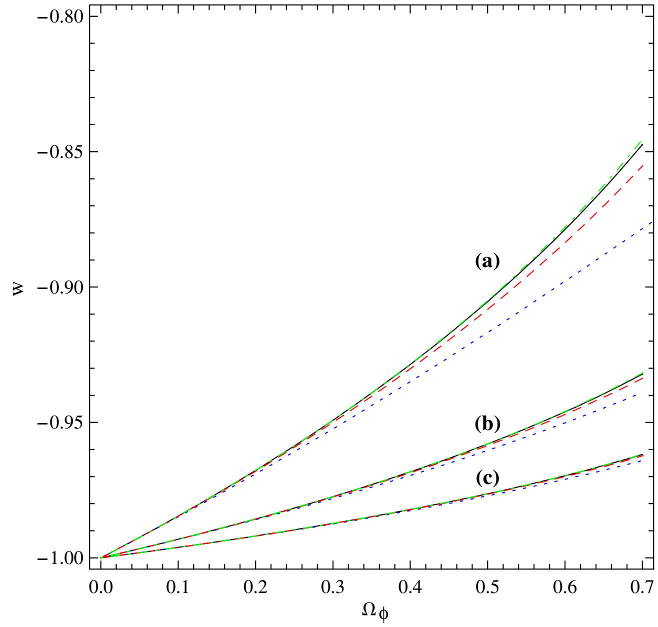

FIG. 2 (color online). Plot of dark energy equation of state parameter w versus Ω_ϕ for $0 \le \Omega_\phi \le 0.7$ in the case of different values of λ_0 for the nonphantom case, i.e. $\epsilon = 1$. The curves are for the potentials $V(\phi) = \phi^{-3}$ (dot-dashed curve), $V(\phi) = \phi^{-2}$ (dashed curve), and $V(\phi) = \phi^{-1}$ (dotted curve). The black solid line is for our analytical approximation (17). The sets (a), (b), and (c) are for $\lambda_0 = 1$, $2/3$, and $1/2$ respectively.

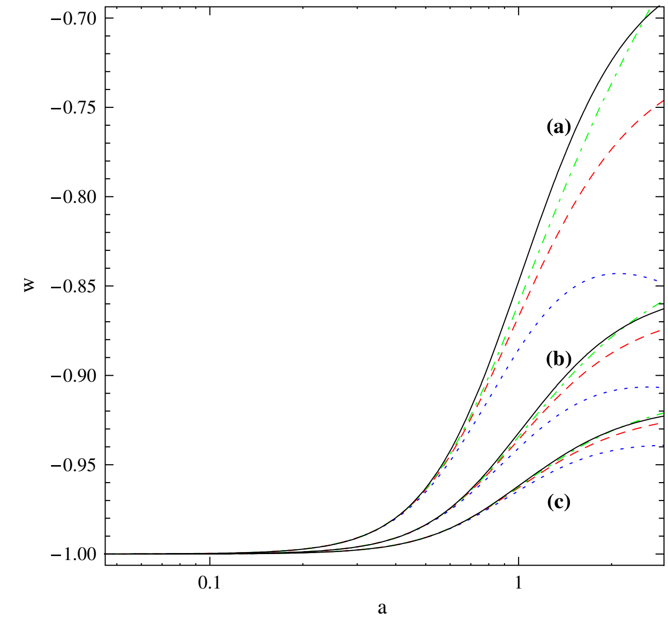

FIG. 4 (color online). Plot of dark energy equation of state parameter w versus a in the case of different values of λ_0 for the nonphantom case, i.e. $\epsilon = 1$. The curves are for the potentials $V(\phi) = \phi^{-3}$ (dot-dashed curve), $V(\phi) = \phi^{-2}$ (dashed curve), and $V(\phi) = \phi^{-1}$ (dotted curve). The black solid line is for our analytical approximation (17) together with (20). The sets (a), (b), and (c) are for $\lambda_0 = 1$, $2/3$, and $1/2$ respectively.

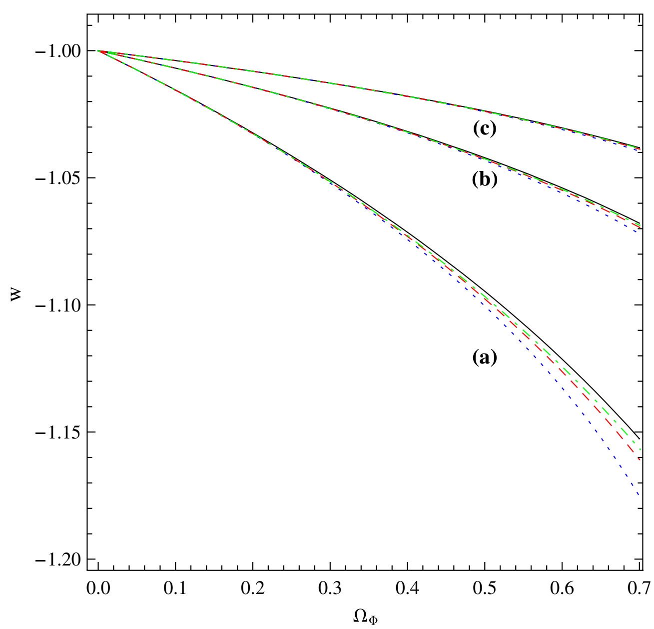

FIG. 3 (color online). Plot of dark energy equation of state parameter w versus Ω_ϕ for $0 \le \Omega_\phi \le 0.7$ in the case of different values of λ_0 for the phantom case, i.e. $\epsilon = -1$. The curves are for the potentials $V(\phi) = \phi^{-3}$ (dot-dashed curve), $V(\phi) = \phi^{-2}$ (dashed curve), and $V(\phi) = \phi^{-1}$ (dotted curve). The black solid line is for our analytical approximation (17). The sets (a), (b) and (c) are for $\lambda_0 = 1$, $2/3$, and $1/2$ respectively.

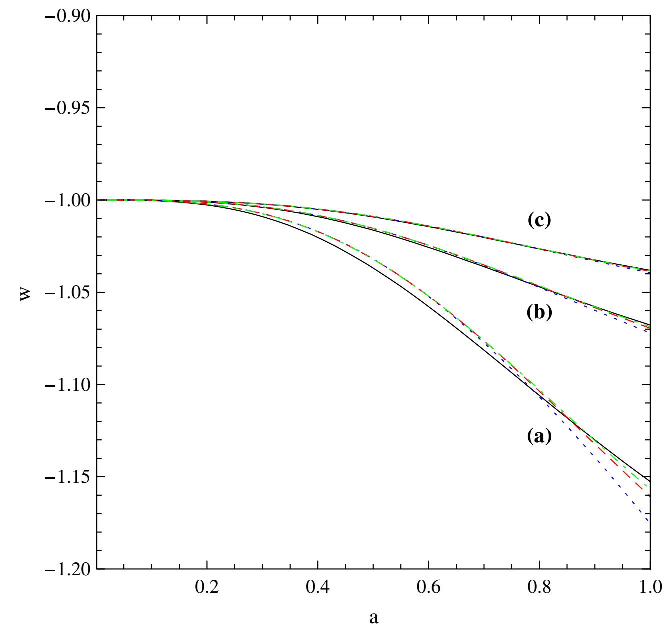

FIG. 5 (color online). Plot of dark energy equation of state parameter w versus a in the case of different values of λ_0 for phantom case, i.e. $\epsilon = -1$. The curves are for the potentials $V(\phi) = \phi^{-3}$ (dot-dashed curve), $V(\phi) = \phi^{-2}$ (dashed curve), and $V(\phi) = \phi^{-1}$ (dotted curve). The black solid line is for our analytical approximation (17) together with (20). The sets (a), (b), and (c) are for $\lambda_0 = 1$, $2/3$, and $1/2$ respectively.

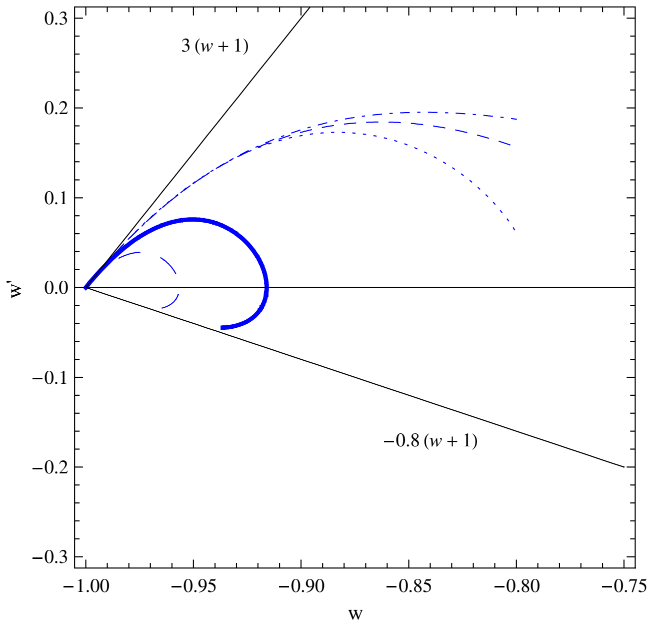

FIG. 6 (color online). The graph shows w-w' phase space occupied by the fields. The upper bound and the lower bound correspond to $3(1+w)$ and $-0.8(1+w)$ respectively. The curves are for the potentials $V(\phi) = \phi^{-3}$ (dot-dashed curve), $V(\phi) = \phi^{-2}$ (short dashed curve), $V(\phi) = \phi^{-1}$ (dotted curve), $V(\phi) = \phi^{-0.2}$ (thick curve), and $V(\phi) = \phi^{-0.1}$ (long dashed curve). The two thin lines represent the upper and lower bound for the thawing models. The corresponding bounds are also specified.

$$\Omega_\phi = [1 + (\Omega_{\phi 0}^{-1} - 1)a^{-3}]^{-1}, \tag{19}$$

where $\Omega_{\phi 0}$ is the present-day value of Ω_ϕ. Equations (17) and (19) give the complete behavior for the equation of state $w(a)$ for tachyon fields with potentials satisfying the slow-roll conditions (15). One can also express the parameter λ_0 in terms of the present-day value w_0 of the equation of state which is quite straightforward. This behaviors are shown in Figs. 4 and 5 for nonphantom and phantom cases.

Similar to the case of thawing quintessence, nonphantom tachyon models are restricted to a part of the w'-w plane. To specify the limits, let us define a parameter X

$$X = -\frac{\ddot{\phi}}{H\dot{\phi}w} = -\frac{w'}{2w(1+w)} \rightarrow w' = -2Xw(1+w).$$

Since the Hubble parameter is determined by the matter dominated regime in the beginning of evolution, we find that $X = -3/2w \leq 3/2$ as $w \geq -1$ which leads to the upper limit, $w' < 3(1+w)$. The lower bound on w' is estimated numerically (demanding that at present $\Omega_\phi \leq 0.8$) as $w' > -0.8(1+w)$ giving rise to the permissible region of w'-w plane

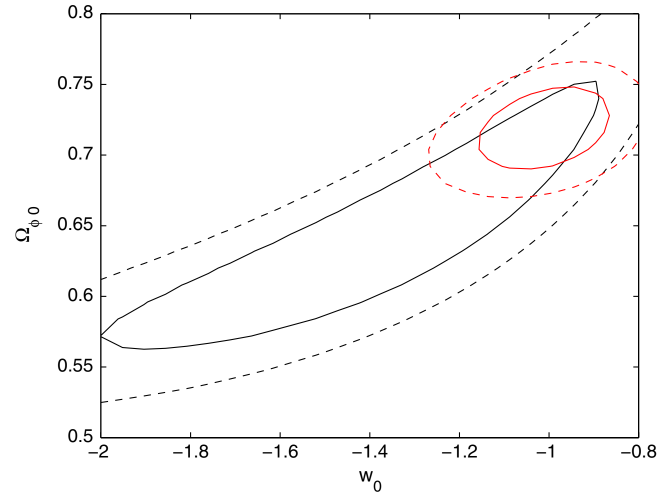

FIG. 7 (color online). Constraints in w_0-$\Omega_{\phi 0}$ parameter space using Union08 compilations of SN data and BAO data. Black lines (larger contours) are for SN data only while red lines (smaller contours) are for SN + BAO data. Solid lines are for 1σ contour intervals while dashed lines are for 2σ contour intervals.

$$-0.8(1+w) < w' < 3(1+w). \tag{20}$$

In Fig. 6 we have shown this permissible region together with the actual behavior for different potentials.

III. OBSERVATIONAL CONSTRAINT

The solution given by Eqs. (17) and (19) for the equation of state parameter w versus the scale factor a for tachyon field under slow-roll conditions is exactly similar to that for a canonical scalar field as obtained earlier in [18,19]. They have also constrained the two parameters w_0 and $\Omega_{\phi 0}$ of the model using the SNLS (Supernova Legacy Survey) [20] and Baryon Acoustic Oscillation (BAO) data [21]. At present, we have the Union08 compilation of the supernova type Ia data which contains around 307 data points [22]. This is world's published first heterogeneous supernova data set containing a large sample of data from SNLS, the Essence survey, high redshift supernova data from the Hubble Space telescope, as well as several small data sets. We use this data set together with the BAO data from SDSS (Sloan Digital Sky Survey) [21]. The 1σ and 2σ contour intervals for our model have been shown in Fig. 7. From the figure, it is clear that one cannot distinguish the cosmological constant with a thawing dark energy model with present data although the phantom dark energy models are preferred.

IV. CONCLUSIONS

In this paper we have examined the DBI system with a phenomenologically motivated class of runaway potentials. In general, the tachyon dynamics crucially depends upon the asymptotic behavior of the potential $V(\phi)$ at large values of ϕ. The inverse square potential gives rise to constant equation of state which is determined by the slope of the potential $w = -1 + \lambda^2/2$. We analyzed the class of tachyon potentials with dark energy and dark matter as late time attractors. Models in which $V(\phi)$ decrease faster than ϕ^{-2} can give rise to transient dark energy near the top of the potential and then mimic dark matter as a late time attractor. Since ρ_ϕ for the tachyon field scales slower than matter, its energy density for a viable cosmic evolution should be fixed around ρ_Λ at earlier epochs allowing the field to freeze due to large Hubble damping. Thus all three classes of tachyon models belong to the thawing type. The data available at present allow one to carry out investigations around the present epoch with $\gamma_\phi \ll 1$. As soon as ρ_ϕ becomes comparable to matter density, the field begins to evolve. The equation of state improves slightly starting from $w(\phi) = -1$. Hence, the slope of the potential does not change appreciably, which we confirmed numerically. In the limit of small adiabatic index of ϕ assuming λ to be constant, we have shown that the resulting evolution equations are the same as in the case of quintessence, which can be solved analytically. Our simulation shows that the approximation is very close to the numerical results for $\lambda < 1$ around the present epoch. Deviations are possible in the far future. We therefore conclude that tachyon dynamics is difficult to distinguish from quintessence at least in the near future. We also extended our analysis to the case of the phantom tachyon. Again in the region of interest, we find that the phantom tachyon model is difficult to distinguish from the ordinary phantom field. We also constrained the parameters w_0 and $\Omega_{\phi 0}$ for our model using the latest supernovae data along with baryon acoustic oscillation BAO data. Our analysis shows some preference for phantom energy.

The fact that all the scalar field dark energy models have a unique equation of state as long as they are in the slow-roll regime makes a strong case for the $w(a)$ given by Eqs. (17) and (19). It does not matter whether the scalar field has a canonical or noncanonical kinetic term. It is also the same for nonphantom or phantom scalar fields. We hope that this equation of state behavior for the dark energy will be considered seriously while fitting with the observational data coming from future experiments.

ACKNOWLEDGMENTS

A. A. S. acknowledges the financial support provided by the University Grants Commission, Government of India, through the major research project grant (Grant No. 33-28/2007(SR)).

[1] V. Sahni and A. A. Starobinsky, Int. J. Mod. Phys. **D9**, 373 (2000); S. M. Carroll, Living Rev. Relativity **4**, 1 (2001); T. Padmanabhan, Phys. Rep. **380**, 235 (2003); P. J. E. Peebles and B. Ratra, Rev. Mod. Phys. **75**, 559 (2003); E. V. Linder, J. Phys. Conf. Ser. **39**, 56 (2006); arXiv:hep-th/0603057; L. Perivolaropoulos, AIP Conf. Proc. **848**, 698 (2006); N. Straumann, arXiv:gr-qc/0311083.

[2] E. J. Copeland, M. Sami, and S. Tsujikawa, Int. J. Mod. Phys. **D15**, 1753 (2006).

[3] E. V. Linder, Gen. Relativ. Gravit. **40**, 329 (2008); J. Frieman, M. Turner, and D. Huterer, Annu. Rev. Astron. Astrophys. **46**, 385 (2008); Robert R. Caldwell and Marc Kamionkowski, arXiv:0903.0866; A. Silvestri and Mark Trodden, arXiv:0904.0024.

[4] I. Zlatev, L. M. Wang, and P. J. Steinhardt, Phys. Rev. Lett. **82**, 896 (1999); P. J. Steinhardt, L. M. Wang, and I. Zlatev, Phys. Rev. D **59**, 123504 (1999); L. Amendola, Phys. Rev. D **62**, 043511 (2000).

[5] C. Armendariz-Picon, V. Mukhanov, and P. J. Steinhardt, Phys. Rev. Lett. **85**, 4438 (2000); Phys. Rev. D **63**, 103510 (2001); T. Chiba, T. Okabe, and M. Yamaguchi, Phys. Rev. D **62**, 023511 (2000).

[6] R. Kallosh, J. Kratochvil, A. Linde, E. Linder, and M. Shmakova, J. Cosmol. Astropart. Phys. 10 (2003) 015; Y. WangJ. KratochvilA. LindeE. LinderM. ShmakovaJ. Cosmol. Astropart. Phys.12 (2004) 006; P. P. Avelino, C. J. A. P. Martins, and J. C. R. E. Oliveira, Phys. Rev. D **70**, 083506 (2004); P. P. Avelino, Phys. Lett. B. **611**, 15 (2005).

[7] A. Sen, J. High Energy Phys. 04 (2002) 048; 07 (2002) 065; Mod. Phys. Lett. A **17**, 1797 (2002); Phys. Scr. **T117**, 70 (2005).

[8] A. Sen, J. High Energy Phys. 10 (1999) 008; M. R. Garousi, Nucl. Phys. **B584**, 284 (2000); **B647**, 117 (2002); J. High Energy Phys. 05 (2003) 058; E. A. Bergshoeff, M. de Roo, T. C. de Wit, E. Eyras, and S. Panda, J. High Energy Phys. 05 (2000) 009; J. Kluson, Phys. Rev. D **62**, 126003 (2000); D. Kutasov and V. Niarchos, Nucl. Phys. **B666**, 56 (2003).

[9] E. J. Copeland, M. R. Garousi, M. Sami, and S. Tsujikawa, Phys. Rev. D **71**, 043003 (2005).

[10] S. Tsujikawa and M. Sami, Phys. Lett. B **603**, 113 (2004); M. Sami, N. Savchenko, and A. Toporensky, Phys. Rev. D **70**, 123528 (2004).

[11] L. P. Chimento, Monica Forte, G. M. Kremer, and M. O. Ribas, arXiv:0809.1919; W. Chakraborty and Ujjal Debnath, Astrophys. Space Sci. **315**, 73 (2008); I. Ya. Aref'eva and A. S. Koshelev, J. High Energy Phys. 09 (2008) 068; Zong-Kuan Guo and Nobuyoshi Ohta, J. Cosmol. Astropart. Phys. 04 (2008) 035; M. R. Setare, Phys. Lett. B **653**, 116 (2007); Z. Keresztes, L. A. Gergely, V. Gorini, U. Moschella, and A. Yu. Kamenshchik, Phys.

Rev. D **79**, 083504 (2009).
[12] T. Padmanabhan, Phys. Rev. D **66**, 021301 (2002).
[13] G. N. Felder, Lev Kofman, and A. Starobinsky, J. High Energy Phys. 09 (2002) 026.
[14] J. S. Bagla, H. K. Jassal, and T. Padmanabhan, Phys. Rev. D **67**, 063504 (2003).
[15] L. R. W. Abramo and F. Finelli, Phys. Lett. B **575**, 165 (2003).
[16] J. M. Aguirregabiria and R. Lazkoz, Phys. Rev. D **69**, 123502 (2004).
[17] Z. K. Guo and Y. Z. Zhang, J. Cosmol. Astropart. Phys. 08 (2004) 010.
[18] R. J. Scherrer and A. A. Sen, Phys. Rev. D **77**, 083515 (2008).
[19] R. J. Scherrer and A. A. Sen, Phys. Rev. D **78**, 067303 (2008).
[20] T. Davis *et al.*, Astrophys. J. **666**, 716 (2007).
[21] D. J. Eisenstein *et al.*, Astrophys. J. **633**, 560 (2005).
[22] M. Kowalski *et al.*, Astrophys. J. **686**, 749 (2008).